EC Accepts, published online ahead of print on 18 April 2014
Eukaryotic Cell doi:10.1128/EC.00341-13
Copyright © 2014, American Society for Microbiology. All Rights Reserved.

EC Accepts published online ahead of print

1 *Trypanosoma cruzi* Bromodomain Factor 3 (*Tc*BDF3) binds acetylated α tubulin and
2 concentrates in the flagellum during metacyclogenesis
3
4
5 Victoria Lucia Alonso[a,b], Gabriela Vanina Villanova[a,b], Carla Ritagliati[b], María Cristina
6 Machado Motta[c], Pamela Cribb[a,b] and Esteban Carlos Serra[a,b]#
7
8 Facultad de Ciencias Bioquímicas y Farmacéuticas, Universidad Nacional de Rosario (UNR).
9 Rosario, Argentina[a]; Instituto de Biología Molecular y Celular de Rosario (IBR), CONICET.
10 Rosario, Argentina[b]; Laboratório de Ultraestrutura Celular Hertha Meyer, Instituto de Biofísica
11 Carlos Chagas Filho, Universidade Federal do Rio de Janeiro. Rio de Janeiro, Brazil[c].
12
13 Running head: *T. cruzi* bromodomain 3 binds acetylated α tubulin
14
15 #Address correspondence to Esteban C. Serra: eserra@fbioyf.unr.edu.ar
16
17
18
19
20
21
22
23
24

EC Accepts published online ahead of print

25 **Abstract**

26 Bromodomains are highly conserved acetyl-lysine binding domains found mainly in proteins
27 associated with chromatin and nuclear acetyltransferases. The *Trypanosoma cruzi* genome
28 encodes at least four Bromodomain Factors (*Tc*BDFs). We describe here Bromodomain
29 Factor 3 (*Tc*BDF3), a bromodomain-containing protein localized in the cytoplasm. *Tc*BDF3
30 cytolocalization was determined using purified antibodies by western blot analysis (WB) and
31 immunofluorescence (IF) in all life cycle stages of *T. cruzi*. In epimastigotes and amastigotes
32 it was detected in the cytoplasm, the flagellum and the flagellar pocket and in trypomastigotes
33 only in the flagellum. Subcellular localization of *Tc*BDF3 was also determined by digitonin
34 extraction, ultrastructural immunocytochemistry and expression of *Tc*BDF3 fused to Cyan
35 Fluorescent Protein (CFP). Tubulin can acquire different posttranslational modifications
36 (PTMs), which modulate microtubules functions. Acetylated α tubulin has been found in the
37 axoneme of flagella and cilia as well as in the subpellicular microtubules of Trypanosomatids.
38 *Tc*BDF3 and acetylated α tubulin partially co-localized in isolated cytoskeletons and flagella
39 from *T. cruzi* epimastigotes and trypomastigotes. Interaction between the two proteins was
40 confirmed by co-immunoprecipitation and far western blot assays with synthetic acetylated α
41 tubulin peptides and recombinant *Tc*BDF3.

42
43
44
45
46
47
48

EC Accepts published online ahead of print

49 **Introduction**

50 *Trypanosoma cruzi* is a protozoan parasite and the causative agent of Chagas disease. It has
51 a complex life cycle that alternates between two hosts and at least four distinct developmental
52 stages. Amastigotes and bloodstream trypomastigotes are present in the mammalian host
53 whereas epimastigotes and the infective metacyclic trypomastigotes are present in the insect
54 vector (from the Triatominae and Reduviidae family). The differentiation event, from
55 epimastigotes to metacyclic trypomastigotes occurring inside the insect, is called
56 metacyclogenesis. This process can be induced *in vitro* using artificial media that resemble
57 the conditions inside the vector and occurs spontaneously in old epimastigote cultures (1).
58 Trypanosomatids are characterized by the presence of a particular cytoskeleton responsible
59 for the modulation of cell shape between the different life cycle stages and for motility and
60 attachment to the host cell surface (2). These parasites present a layer of microtubules (MT),
61 the subpellicular microtubules, located below the plasma membrane and a flagellum with a
62 typical 9+2 pattern of axonemal microtubules. The flagellum emerges from a membrane
63 invagination called the flagellar pocket (FP). Four cytoplasmic microtubules are nucleated
64 close to the basal body and run around the FP and along the entire flagellum attachment
65 zone (FAZ) to the anterior cellular pole. The FP lacks the layer of subpellicular microtubules
66 and is the place where endocytosis and exocytosis occur (3).
67 Microtubules can acquire a variety of evolutionary conserved posttranslational modifications
68 (PTM). It was proposed that these modifications dictate the recruitment of protein complexes
69 that might regulate microtubule-based functions in different cellular locations (Reviewed by (4-
70 7)). Acetylation occurs on Lysine 40 of α tubulin (4-5) and it was thought that MT stabilization
71 was a consequence of this PTM (6-7). However, it was recently demonstrated that acetylation
72 of MTs do not necessarily affect their stability (8-9).

EC Accepts published online ahead of print

73 In Trypanosomatids, acetylated α tubulin is found in the subpellicular microtubules and in the
74 flagella of *T. cruzi* and *T. brucei* (10-11). This PTM is also present in the ephemeral
75 microtubules of the mitotic spindle of *T. brucei* (11). The presence of acetylated α tubulin in
76 early mitotic spindles in several organisms and the fact that protozoa like *T. brucei* and *T.*
77 *cruzi* exhibit global α tubulin acetylation reinforces the idea that this PTM is not restricted to
78 stable MTs (Reviewed by (12)).
79 Although tubulin acetylation has been described a long time ago, the enzymes responsible for
80 this reversible modification have recently started to emerge. The first tubulin deacetylase
81 described in mammals was HDAC6 (class II histone deacetylase), which can also modify
82 other non-nuclear proteins (13). SIRT2, is a NAD-dependent deacetylase (class III histone
83 deacetylase or Sirtuin) capable of modifiying α tubulin (14). In the *Trypanosoma cruzi* genome
84 (http://tritrypdb.org/tritrypdb/) there are two coding sequences (CDSs) for histone
85 deacetylases homologous to HDAC6 and two CDSs for Sirtuins. The *Leishmania infantum*
86 Sirtuin (*Li*SIR2RP1) is a NAD-dependent deacetylase and ADP-ribosyltransferase capable of
87 deacetylating α tubulin (15). Also, there are two tubulin acetyltransferases described until
88 now. The ELP3 subunit of the Elongator complex is known to modify microtubules of the
89 cortical neurons (16) and αTAT-1, which has recently been proposed as the mayor α tubulin
90 K40 acetyltransferase in mammals and nematodes (17). The *Trypanosoma cruzi* genome
91 contains two sequences homologous to ELP3. In *Trypanosoma brucei, Tb*ELPa and b have
92 been reported (18). Also, a putative sequence homologous to αTAT-1 is present in
93 trypanosomatids but has not been characterized yet.
94 Bromodomains are conserved protein modules, capable of binding acetylated lysines and
95 found in proteins associated with chromatin and in nearly every nuclear histone
96 acetyltransferase. They have an atypical left-handed four-helix bundle structure (helixes α_A,

EC Accepts published online ahead of print

97 α_B, α_C, and α_Z) connected by two loops (loop ZA and loop BC) that constitute the surface
98 accessible hydrophobic pocket where the acetyl-lysine binding site is located (19).
99 Bromodomains can interact with other proteins in an acetylation-dependent manner and form
100 multi-subunit complexes (20). The Bromodomain is considered a nuclear domain but a small
101 number of bromodomain-containing proteins have a dual nuclear-cytosolic localization (21-
102 23).
103 Genes coding for putative bromodomain containing factors (BDFs) were found in the TriTryp
104 genomes (*Trypanosoma brucei, Trypanosoma cruzi and Leishmania* ssp.) (24). We have
105 previously characterized *Tc*BDF2, which binds histone H4 (25). Here we describe
106 Bromodomain Factor 3 from *Trypanosoma cruzi* (*Tc*BDF3), the first exclusively non-nuclear
107 bromodomain-containing protein reported so far. *Tc*BDF3 is expressed in all life cycle stages
108 and interacts with acetylated α tubulin, the major component of the flagellar and subpellicular
109 microtubules. In both metacyclic and bloodstream trypomastigotes, *Tc*BDF3 was found
110 concentrated in the flagellum and in the flagellar pocket region. Even though the precise
111 function of *Tc*BDF3 remains unrevealed, the results presented herein suggest a participation
112 of this bromodomain factor in cytoskeleton dynamics.
113
114 **Materials and Methods**
115 Ethics Statement
116 All experiments were approved by the Institutional Animal Care and Use Committee of the
117 School of Biochemical and Pharmaceutical Sciences (National University of Rosario,
118 Argentina) and conducted according to specifications of the US National Institutes
119 of Health guidelines for the care and use of laboratory animals.
120 Cell culture

EC Accepts published online ahead of print

121 The Vero cell line was routinely cultivated in DMEM medium (Gibco) supplemented with 10%
122 heat inactivated Fetal Calf Serum (FCS), 0.15% (w/v) $NaHCO_3$, 100 U ml^{-1} penicillin and 100
123 mg ml^{-1} streptomycin at 37°C in a humid atmosphere containing 5% CO_2.
124 Parasites
125 Epimastigotes of *T. cruzi* Dm28c strain were cultured in liver infusion-tryptose medium (LIT)
126 (26) supplemented with 10% FCS at 28°C. The parasites were kept in exponential growth
127 phase by sub-culturing every three days. Intracellular forms and trypomastigotes were
128 obtained by infecting Vero cells with trypomastigotes as previously described (27-28).
129 To obtain metacyclic trypomastigotes, epimastigotes were differentiated *in vitro* following the
130 procedure described by Contreras and co-workers (1) using chemically defined conditions
131 (TAU3AAG medium). Culture supernatants were collected after 24, 48 and 72 h of incubation
132 in TAU3AAG medium.
133 Plasmid construction and expression of *Tc*BDF3
134 *Tc*BDF3 gene was amplified by PCR using BDF3Fw
135 (5'AAGGATCCATGGGCTCTACGGGTCGG) and BDF3Rv
136 (5'AACTCGAGCCTCGTCCTCCACCGCC) oligonucleotides. *Tc*BDF3ΔC fragment was
137 amplified using BDF3Fw and BDF3ΔCRv (5´AACTCGAGTGCTCTTCCGCAAGACGCTCC)
138 oligonucleotides. Proofreading DNA polymerase was used. DNA purified from cultured *T.*
139 *cruzi* epimastigotes served as template.
140 PCR products were inserted into pCR 2.1TOPO® vector (Invitrogen) and sequenced.
141 *Tc*BDF3 and *Tc*BDF3ΔC coding regions were inserted into a pENTR3C vector (Gateway
142 system® Invitrogen) and then transferred by recombination to pDEST17 (Gateway system®
143 Invitrogen) and p*Tc*CFPN (29) using LR clonase II enzyme mix (Invitrogen) to generate
144 Histidine tag and cyan fluorescent protein (CFP) fusions. pDEST17-*Tc*BDF3 was transformed

EC Accepts published online ahead of print

145 into *Escherichia coli* BL21 pLysS and the recombinant protein (fused to a His-tag) was
146 obtained by induction with 0.5 mM IPTG for 3 h at 37°C. The protein was purified by affinity
147 chromatography using a Ni-NTA agarose resin (Qiagen) following the manufacturer's
148 instructions. The secondary structure of recombinant *Tc*BDF3 was measured by circular
149 dicroism.

150 Polyclonal antibodies

151 Rabbit and mouse polyclonal antisera against *Tc*BDF3 were obtained by inoculating
152 subcutaneously recombinant *Tc*BDF3 three times. First using complete Freund's adjuvant
153 and with incomplete adjuvant the following times. Specific antibodies were purified from the
154 antisera obtained by chromatography through a Ni-NTA agarose column containing cross-
155 linked *Tc*BDF3-His. Antibodies were eluted with 100 mM triethylamine pH 11, neutralized to
156 pH 7 and stored at 4°C or at -20°C with 50% glycerol. The purified antibodies specificity was
157 tested by western blot assays.

158 Protein extracts

159 Exponentially growing epimastigotes were washed twice with cold PBS, pellets were
160 resuspended in lysis buffer (20 mM Hepes, 8M Urea) and incubated for 30 minutes at room
161 temperature with gentle agitation. Insoluble debris was eliminated by centrifugation. The
162 same procedure was applied to amastigote and trypomastigote cellular pellets. To obtain
163 nuclear extracts, exponentially growing epimastigotes were washed with PBS, lysed in
164 hypotonic buffer A (10 mM HEPES pH 8, 50 mM NaCl, 1 mM EDTA, 5 mM $MgCl_2$, 1% v/v
165 Nonidet P-40, 1 mM phenylmethylsulphonyl fluoride (PMSF), aprotinin, 0.25% Triton X-100),
166 5% v/v glycerol was added and the pellet was collected by centrifugation. Pellets were
167 washed with buffer B (10 mM HEPES pH 8, 140 mM NaCl, 1 mM EDTA, 5 mM MgCl2 5% v/v
168 glycerol, 1 mM PMSF, 10 μg ml^{-1} aprotinin) and incubated for 10 min on ice. Nuclei were

EC Accepts published online ahead of print

169 collected by centrifugation and resuspended in Buffer C (10 mM HEPES pH 8, 400 mM NaCl,
170 0.1 mM EDTA, 0.5 mM DTT, 5% v/v glycerol, 1 mM PMSF, 10 µg ml^{-1} aprotinin), incubated
171 for 1 h on ice and sonicated. This extraction was repeated three times and supernatants were
172 precipitated with 20% trichloroacetic acid (TCA) overnight at 4 C°.
173 *Trypanosoma cruzi* cytoskeleton enriched extracts were prepared as previously described by
174 Schneider and co-workers (11). Briefly, cells were harvested, washed twice with PBS and
175 incubated with EB buffer (50 mM HEPES, 5 mM EGTA, 1 mM $MgSO_4$, 0,1 mM EDTA, 2 mM
176 $MgCl_2$, 0.1% Triton-X100 and Protease Inhibitor Cocktail set I, Calbiochem) on ice for 30
177 minutes. The lysate was centrifuged at 10,000 x g for 15 minutes and the supernatant, which
178 contained soluble proteins, was named Sn1. The remaining pellet was incubated with EB
179 buffer supplemented with 1M NaCl on ice for 5 minutes, sonicated and centrifuged at 20,000
180 x g for 15 minutes. The supernatant obtained contained soluble flagellar and cytoskeletal
181 proteins (Sn2). The remaining pellet (P) contained insoluble flagellar and cytoskeletal
182 proteins. Supernatants were precipitated with 20% TCA overnight at 4 °C.
183 For immunoprecipitation assays cells were incubated with 1 mM DSP
184 (dithiobis[succinimidylpropionate]) (Thermo Scientific) for 2 hours on ice. This reagent was
185 used to cross-link protein complexes within the cell. After incubation the reaction was stopped
186 with 20 mM Tris, pH 7.5. Then the cells were harvested and incubated with EB buffer
187 supplemented with 1 M NaCl on ice for 30 minutes. The lysate was centrifuged at 10,000 x g
188 for 15 minutes and the supernatant obtained was used to perform co-immunoprecipitation
189 experiments.
190 Western blot and slot blot
191 Protein extracts (30-50 µg per well) were separated by SDS-PAGE and transferred to
192 nitrocellulose membranes. Transferred proteins were visualized with Ponceau S. Membranes

EC Accepts published online ahead of print

193 were treated with 10 % non-fat milk in PBS for 2 hours and then incubated with specific
194 antibodies diluted in PBS for 3 hours. The antibodies used were: polyclonal rabbit and mouse
195 anti-*Tc*BDF3; monoclonal mouse anti-acetylated α tubulin antibody clone 6-11B-1 (Sigma
196 Aldrich); monoclonal mouse anti-trypanosome α tubulin clone TAT-1 (gift from K. Gull,
197 University of Oxford, England, UK.); mouse anti-paraflagellar rod protein 2 (gift from Ariel
198 Silber, University of São Pablo, Brazil); mouse anti-*Trypanosoma cruzi* Histone H4 (gift from
199 Sergio Shenkman, Universidade Federal de São Paulo, Brazil); rabbit anti-*Trypanosoma cruzi*
200 High Mobility Group B (*Tc*HMGB) (30) and anti- *Trypanosoma cruzi* Bromodomain factor 2
201 (*Tc*BDF2) (25). Bound antibodies were detected using peroxidase labelled anti-mouse or anti-
202 rabbit IgGs (GE Healthcare) and ECL Prime (GE Healthcare) according to manufactures
203 protocol.

204 Slot Blot was performed immobilizing 10 µg of α tubulin (PDGAMPSDKTIGVEDDA;
205 Genscript), α tubulin acetylated on lysine 40 (PDGAMPSDKacTIGVEDDA; Genscript) and
206 histone H4 acetylated on lysine 14 (AKGKKSGEAKGTQKacRQ; (31)) synthetic peptides onto
207 nitrocellulose membranes. The membranes were incubated with recombinant His-tagged
208 *Tc*BDF3 or *Tc*BDF2 for 3 hours (0.5 µg/ml). Bound proteins were visualized using anti-
209 Histidine antibodies (GE Healthcare) and detected as mentioned above.

210 Subcellular localization of *Tc*BDF3 by digitonin extraction

211 Parasites in exponential phase were collected, washed and resuspended in buffer A (20 mM
212 Tris–HCl, pH 7.2 with 225 mM sucrose, 20 mM KCl, 10 mM KH_2PO_4, 5 mM $MgCl_2$, 1 mM
213 Na_2EDTA and 1 mM DTT) at a concentration of 1 mg ml^{-1} protein and supplemented with
214 digitonin (0-1 mg) (final volume of 1 ml for each digitonin concentration). The resuspended
215 parasites were incubated at 28 °C for 20 min before being centrifuged at 14,000 x g for 2 min
216 at 4 °C. The enzymatic activities of Alpha-hydroxiacid dehydrogenase (αHAdH) (cytosolic

EC Accepts published online ahead of print

217 marker) and Malate dehydrogenase (MdH) (glycosomal and mitochondrial marker) were
218 determined in the supernatant (S) and occasionally in the cell pellet (P) in the presence of
219 0.1% (v/v) Triton X-100 and 150 mM NaCl. To measure the enzymatic activity of αHAdH the
220 extracts were incubated with 4 ul of 0.5 mM NADH, 7 ul of 1 mM Phenilpyruvate, 2 ul 20%
221 (v/v) Tritón X-100 and 40 ul of the protein extract in 10 mM Tris-HCl pH 8. The percentage of
222 activity was determined spectrophotometrically by measuring the oxidation of NADH
223 (ε339nm=6220 M^{-1} cm^{-1}) at 340 nm. To measure the enzymatic activity of MdH the extracts
224 were incubated with 5 ul of 0.5 mM NADH, 10 ul of 1 mM Oxalacetate, 2 ul 20% (v/v) Tritón
225 X-100 and 20 ul of the protein extract in 10 mM Tris-HCl pH 8. The percentage of activity was
226 determined spectrophotometrically by measuring the oxidation of NADH (ε339nm=6220 M^{-1}
227 cm^{-1}) at 340 nm.
228 Equal volumes of selected S and P fractions were subjected to SDS-PAGE, blotted onto
229 nitrocellulose membranes and probed with specific antibodies. The antibodies used were:
230 Anti-Tyrosine Amino Transferase antibodies (*Tc*TAT), anti-Glycosomal Malate
231 Dehydrogenase (*Tc*MdHglyc), anti-Mitochondrial Malate Dehydrogenase (*Tc*MdHmit)
232 antibodies (all of them where a gift from Cristina Nowicki, Universidad de Buenos Aires,
233 Argentina), anti-paraflagellar rod 2 (*Tc*PAR2) antibodies and mouse monoclonal anti-
234 trypanosome α tubulin clone TAT-1 (α tubulin).
235 Ultrastructural Immunocytochemistry
236 Parasites were fixed in 0.3% glutaraldehyde, 4% formaldehyde and 1% picric acid diluted in
237 0.1 M cacodylate buffer at pH 7.2 and then dehydrated at 20 °C using a graded acetone series
238 and progressively infiltrated with Unicryl at lower temperatures. The polymerization of the
239 resin was carried out in BEEM capsules at 20 °C for 5 days under UV light. Ultra-thin sections
240 were obtained in a Leica ultramicrotome (Reichert Ultracuts) and the grids containing the

EC Accepts published online ahead of print

241 sections were incubated with 50 mM NH_4Cl for 30 min. The grids were then incubated with
242 blocking solution (3.5% BSA, 0.5% teleostean gelatine, 0.02% Tween -20 diluted in PBS, pH
243 8.0) for 30 min and finally with goat serum diluted in blocking solution (1:200). Grids
244 containing ultra-thin sections were incubated for 1 h with anti-*Tc*BDF3 antibodies diluted in
245 blocking solution (1:1) and washed with PBS. Grids were then incubated with gold-labelled
246 goat anti-rabbit IgG diluted 1:200 for 45 min, washed with blocking solution and stained with
247 uranyl acetate and lead citrate for further observation using a Zeiss 900 transmission electron
248 microscope. In control assays, sections were not incubated with the primary anti-serum.
249 Immunocytolocalization
250 Trypomastigotes and exponentially growing epimastigotes were centrifuged, washed twice
251 with PBS, settled on polylisine-coated coverslips and fixed with 4% para-formaldehyde in PBS
252 at room temperature for 20 minutes. Fixed parasites were washed with PBS and
253 permeabilized with 0.2% Triton X-100 in PBS for 10 minutes. After washing with PBS,
254 parasites were incubated with the appropriate primary antibody diluted in 1% BSA in PBS for
255 3 hours at room temperature. In co-localization experiments both antibodies were incubated
256 together. Non-bound antibodies were washed with 0.01% Tween 20 in PBS and then the
257 slides were incubated with fluorescent-conjugated anti-rabbit (Fluorescein, Jackson Immuno
258 Research) or anti-mouse (Rodhamine, Calbiochem) IgG antibodies and 2 µg ml^{-1} of DAPI for
259 1 hour. Alternatively DNA was stained with Propidium Iodide (Invitrogen) according to
260 manufacturer's instructions. The slides were washed with 0.01% Tween 20 in PBS and finally
261 mounted with VectaShield (Vector Laboratories). To analyze intracellular amastigotes, Vero
262 cells monolayers were grown on coverslips and infected with *T. cruzi* trypomastigotes as
263 described above. Three days post infection cultures were washed with PBS and fixed with 4%
264 para-formaldehyde in PBS at room temperature for 20 minutes. The same procedure

EC Accepts published online ahead of print

265 described above was followed for immunodetection. Images were acquired with a confocal
266 Nikon Eclipse TE-2000-E2 microscope using Nikon EZ-C1 Software or an epifluorescence
267 Nikon Eclipse Ni-U microscope. Adobe Photoshop CS and Image J software (32) were used
268 to pseudo-color and process all images.
269 Isolated cytoskeletons and flagellar complexes were obtained for immunocytolocalization as
270 previously described by Sasse and Gull (33) and prepared for immunofluorescence as
271 described above.
272 Transfection of parasites
273 Epimastigotes were grown at 28°C in LIT medium supplemented with 10% FCS, to a density
274 of approximately 3 x 10^7 cells ml^{-1}. Parasites were then harvested by centrifugation at 4,000 x
275 g for 5 min at room temperature, washed once with PBS and resuspended in 0.35 ml of
276 transfection buffer pH 7.5 (0.5 mM $MgCl_2$, 0.1 mM $CaCl_2$ in PBS) to a density of 1 x 10^8 cells
277 ml^{-1}. Cells were then transferred to a 0.2 cm gap cuvette (Biorad) and 15 to 100 µg of DNA
278 was added in a final volume of 40 µl. The mixture was placed on ice for 15 min and then
279 subjected to a pulse of 450 V and 500 µF using GenePulser II (Bio-Rad, Hercules, USA).
280 After electroporation, cells were transferred into 5 ml of LIT medium containing 10% FCS and
281 maintained at room temperature for 15 minutes. Then the cells were incubated at 28°C. After
282 24 h the antibiotic G418 (Genbiotech) was added to an initial concentration of 125 µg ml^{-1}.
283 Then, 72 to 96 hours after electroporation, cultures were diluted 1:5 and antibiotic
284 concentration was doubled. Stable resistant cells were obtained approximately 30 days after
285 transfection.
286 Co-Immunoprecipitation
287 Epimastigotes were grown up to 10^7 parasites ml^{-1} and 10^{10} parasites were used per co-
288 immunoprecipitation experiment. Antibodies anti-*Tc*BDF3 and total IgGs purified from non-

EC Accepts published online ahead of print

289 immunized rabbits were immobilized to magnetic beads (Dynabeads® Invitrogen) following
290 the manufacturer's instructions. The antibody-coupled beads were incubated with the protein
291 extracts for 3 hours at 4 ºC with gentle shaking. Then the beads were washed three times
292 with MME buffer (50 mM HEPES, 5 mM EGTA, 1 mM $MgSO_4$, 0,1 mM EDTA, 2 mM $MgCl_2$)
293 and two times with Last Wash Buffer (30 mM Tris, pH 7.5, 0.02% Tween 20). The protein
294 complexes were eluted with 0,5 M HN_4OH and neutralized. The eluted proteins were
295 separated by SDS-PAGE and then transferred to nitrocellulose membrane for western blot
296 analysis.

297 Molecular exclusion chromatography

298 Molecular exclusion chromatography was carried out using a Superdex 75 column (GE
299 Healthcare) equilibrated with 10 mM sodium phosphate buffer pH 8 at the recommended flow
300 rate of 0.25 ml/min, and the absorbance at 280 nm continuously monitored using an ÄKTA
301 FPLC system (GE Healthcare). The standard curve was constructed using: Lisozime (14,7
302 kDa), GST (27 kDa for the monomeric form and 54 kDa for the dimeric form) and Bovine
303 Serum Albumin (67 kDa). All buffers and samples were filtered (0.45 μm) before use.

304

305 **Results and Discussion**

306 *Trypanosoma cruzi* Bromodomain factor 3 (*Tc*BDF3)

307 *Trypanosoma cruzi* Bromodomain factor 3 (*Tc*BDF3) coding sequence has two almost
308 identical variant haplotypes in the *T. cruzi* genome (TcCLB.510719.70 and TcCLB.509747.110,
309 http://tritrypdb.org/tritrypdb) that encode for a 223 amino acid polypeptide. This coding
310 sequence contains a bromodomain (pfam: PF00439) in its N-terminal portion from R37 to
311 L141 (Supplementary Figure S1A). *Tc*BDF3 has a predicted molecular weight of 24.7 kDa

EC Accepts published online ahead of print

312 and an isolelectric point of 5.2. The C-terminal portion of the sequence shows no similarity
313 with any domain present in databases. However, it is enriched in acidic amino acids (30%
314 glutamic acid + aspartic acid), basic amino acids (37% lysine + arginine) and serine (14%)
315 (Figure S1A). These highly charged low complexity sequences are generally involved in
316 protein-protein interactions.

317 Orthologous genes are present in other trypanosomatids, the *T. brucei* (Tb927.11.10070) and
318 *Leishmania major* (LmjF.36.3360) proteins have a percentage sequence identity of 63% and
319 42% and a similarity of 75.9% and 54.9% respectively with *Tc*BDF3. The similarity between
320 the four *Trypanosoma cruzi* BDFs and bromodomains from other organisms is low, with a
321 percentage of sequence identities always below 20%. However, the amino acids involved in
322 binding the acetyl-lysine are conserved or conservatively substituted, supporting the
323 hypothesis that *Tc*BDF3 has a functional bromodomain (Figure S1B). The secondary
324 structure of *Tc*BDF3 bromodomain region was modelled with the Phyre2 server (34) retriving
325 the characteristic four α-helix pattern of these domains (Figure S1C). When analysed by
326 molecular exclusion chromatography, most of the recombinant *Tc*BDF3 was found to be a
327 dimmer in solution (figure S1D).

328 *Tc*BDF3 is a cytoplasmatic protein

329 To study the expression of *Tc*BDF3 in *Trypanosoma cruzi,* antibodies raised against
330 recombinant protein were purified by affinity chromatography. Western blot analysis with
331 rabbit and mouse antibodies showed a single band of the expected molecular weight in total
332 lysates of *T. cruzi* epimastigotes (Figure S2A). To test the specificity of the anti-*Tc*BDF3
333 antibodies, they were competed with recombinant *Tc*BDF3 and then used in western blot
334 (Figure S2B) and immunofluorescence (Figure S2C) assays.

EC Accepts published online ahead of print

335 *Tc*BDF3 subcellular localization was predicted using pSORTII (http://psort.hgc.jp/form2.html)
336 and Wolf pSORT (http://wolfpsort.org/). Surprisingly, the highest score was assigned to a non-
337 nuclear localization. Also, the TFPP server (Tool for recognizing flagellar proteins in
338 *Trypanosoma brucei*) (35) predicted a flagellar localization for *Tc*BDF3 and its orthologue in
339 *T. brucei* (Tb927.11.10070). Although Tb927.11.10070 has not been identified in the flagellar
340 proteome of *T. brucei* (36-38), it is worth mentioning that due to technical limitations many
341 flagellar proteins fail to be detected or cannot be assigned to the flagellum with certainty by
342 proteomic studies.
343 Then, we evaluated the expression of *Tc*BDF3 in nuclear and non-nuclear epimastigote
344 extracts by western blot analysis. The *Tc*BDF3-specific immunoreactive band was observed
345 only in the non-nuclear fraction. Tyrosine Amino Transferase (*Tc*TAT) (39) is a cytosolic
346 protein and *Tc*HMGB (*Trypanosoma cruzi* High Mobility Group B) (30), *Tc*BDF2 (25) and
347 Histone H4 (40) are all nuclear proteins (Figure 1A). We decided to confirm the non-nuclear
348 localization of this protein through several approaches.
349 First, we performed western blot analysis in subcellular fractions of epimastigotes obtained by
350 digitonin extraction (39). By this approach plasma membranes with high sterol content are
351 specifically permeabilized at low concentration of digitonin, whereas higher concentrations are
352 required to permeabilize glycosomal and mitochondrial membranes (41). Measuring the
353 activity of alpha Hydroxyacid Dehydrogenase (αHAdH) (cytosolic protein) we determined in
354 which fractions the cytosolic (C) content was released (starting at 0.04 mg of digitonin). The
355 Malate Dehydrogenase (MdH) presents a glycosomal and a mitochondrial isoform. Measuring
356 the activity of this enzyme we determined when the glycosomal content (G, starting at 0.2 mg
357 of digitonin) and the mitochondrial content (M, starting at 0.4 mg of digitonin) were released
358 (Figure 1B). The extraction pattern of *Tc*BDF3 was monitored by western blot analysis of

EC Accepts published online ahead of print

359 selected soluble (S) and insoluble (P) fractions (Figure 1C, 0-0.7 mg of digitonin). In
360 agreement with our previous results, *Tc*BDF3 was released at low digitonin concentrations.
361 However, *Tc*BDF3 was not completely extracted in the soluble fraction and an
362 immunoreactive band was observed in all the insoluble fractions, showing a pattern similar to
363 that of PAR2 (a flagellar protein) and α tubulin. These results suggest that *Tc*BDF3 is a
364 cytoplasmatic protein that could also be associated with insoluble proteins in the membrane
365 or cytoskeleton of *T. cruzi*.
366 Then, *Tc*BDF3 was immunolocalized in thin sections of epimastigotes by transmission
367 electron microscopy (TEM). *Tc*BDF3 was not observed over DNA containing structures, such
368 as the nucleus (N) or kinetoplast (K) (Figure 2A-C). *Tc*BDF3 was immunolocalized at the
369 flagellum (F) (Figure 2B, D and F, white arrows), especially in its inner part, which is attached
370 to the cell body. Labelling was also observed dispersed in the cytoplasm and close to the
371 flagellar pocket (FP) (Figure 2A-D, black arrows). In control assays with no primary antibody
372 no immunogold particles were detected (data not shown).
373 Next, *Tc*BDF3 expression during *T. cruzi* life cycle was addressed using epimastigotes,
374 trypomastigotes and amastigotes total protein extracts. A single band of the expected
375 molecular weight was observed for all developmental stages (Figure 3A). The subcellular
376 localization of *Tc*BDF3 was assessed by immunofluorescence microscopy in different stages
377 (Figure 3B). In epimastigotes (E) *Tc*BDF3 was present in the cytoplasm, the flagellum and the
378 flagellar pocket region similar to the pattern obtained by TEM. In amastigotes (A and Ac) we
379 observed an expression pattern similar to epimastigotes. However, the flagellar pocket region
380 was more deeply marked and the plasma membrane appeared to be labelled. Surprisingly, in
381 infective trypomastigotes (T and Tm) *Tc*BDF3 expression pattern changed and was localized
382 exclusively in the flagellum.

383 This change in *Tc*BDF3 localization during the epimastigote-trypomastigote transition was
384 also analysed using N-terminal fusions to the Cyan Fluorescent Protein (CFP). A full length
385 (p*Tc*CFPN-*Tc*BDF3) and a truncated form of *Tc*BDF3, containing the first 131 amino acids
386 (p*Tc*CFPN-*Tc*BDF3ΔC), were over-expressed in epimastigotes. Both fusion proteins were
387 detected in the whole cell body of epimastigotes, in a pattern similar to that observed for
388 *Tc*BDF3 by immunocytolocalization (Figure S3). When transfected parasites were
389 differentiated *in vitro* to trypomastigotes, CFPN-*Tc*BDF3 was found concentrated at the
390 flagellum, as did wild type *Tc*BDF3 (Figure S3A). However, truncated CFPN-*Tc*BDF3ΔC
391 remained dispersed in the cell body (Figure S3B). Expression of CFPN-*Tc*BDF3 and CFPN-
392 *Tc*BDF3ΔC was corroborated by western blot analysis with anti-*Tc*BDF3 antibodies (Figure
393 S3C). These results suggest that the C-terminal portion of *Tc*BDF3 could be important for the
394 flagellar localization of *Tc*BDF3 in trypomastigotes.

395 The presence of a bromodomain containing protein outside the nucleus has been described
396 in other models but always with a dual cytoplasmic-nuclear localization and restricted to some
397 specific mammalian cells (21-23). The existence of a bromodomain factor in the flagellum as
398 described herein, suggests a completely new role for these protein modules. Given that in the
399 last few years several authors, using high resolution mass spectrometry, identified thousands
400 of acetylated proteins involved in a wide variety of cellular processes in different organisms
401 (42-45) it is not unrealistic to think that bromodomains could be playing regulatory roles
402 outside the nuclear compartment. In 2000, Kouzarides proposed that acetylation might rival
403 phosphorylation as a regulator of cell function and that the bromodomain may be analogous
404 to the phosphotyrosine-recognizing SH2 domain (46). The presence of *Tc*BDF3 outside the
405 nucleus opens new perspectives for a possible role of lysine acetylation as a regulatory
406 switch in complex cellular processes as proposed by many authors (47-50).

EC Accepts published online ahead of print

EC Accepts published online ahead of print

407 To study in further detail the differential localization of *Tc*BDF3, *in vitro* metacyclic
408 trypomastigotes were obtained using TAU medium. During the differentiation process
409 between epimastigotes and trypomastigotes, intermediate stages were distinguished and
410 classified based on the position of the kinetoplast, the nucleus and the flagellum as described
411 by Ferreira and co-workers (51) (a schematic representation is shown in Figure 4, right
412 panel). The immunocytolocalization of *Tc*BDF3 and acetylated α tubulin was analyzed in the
413 intermediate differentiation stages (1a, b and c). As it is shown in figure 4, *Tc*BDF3
414 concentrates in the flagellum during metacyclogenesis. As previously reported (10),
415 acetylated α tubulin was detected in the whole cell body in the intermediate stages with no
416 significant changes. However, we observed a partial co-localization of *Tc*BDF3 and acetylated
417 α tubulin in the flagella of the intermediate stages (Figure 4), which strongly suggested that
418 *Tc*BDF3 was associated to the flagellar microtubule structure.

419 *Tc*BDF3 binds to acetylated α tubulin

420 The former results as well as the known ability of bromodomain-containing proteins to bind
421 acetylated proteins led us to think that *Tc*BDF3 could be binding acetylated proteins in the
422 cytoskeleton and flagellum of *T. cruzi*.

423 As already mentioned, microtubules are components of the subpellicular corset, the
424 axoneme, the flagellar pocket and the flagellum attachment zone in trypanosomatids (52).
425 Multiple tubulin isotypes are present in microtubules due to a series of posttranslational
426 modifications. Among all isoforms of α tubulin associated with the *T. cruzi* subpellicular and
427 axonemal microtubules, the acetylated form seems to be predominant (10). Isolated
428 subpellicular microtubules and flagellar complexes from epimastigotes and trypomastigotes
429 were obtained in order to verify the presence of *Tc*BDF3 in these cellular components.
430 *Tc*BDF3 as well as acetylated α tubulin and PAR2 (*a*-PFR, para flagellar rod 2 protein) were

EC Accepts published online ahead of print

431 detected by immunofluorescence (Figure 5). In epimastigotes (E), *Tc*BDF3 was present in
432 discrete regions of the cytoskeleton with a stronger signal in the flagellar pocket region
433 (Figure 5A upper panel). Also it was observed in the flagellum, where it partially co-localized
434 with acetylated α tubulin (Figure 5A lower panel). The protocol performed to obtain isolated
435 flagella, as Sasse and Gull stated in 1988, did not always lead to complete solubilization and
436 a group of subpecculiar MTs attached to basal bodies and forming the flagellar pocket
437 appeared to be resistant to treatment (33). In the enlarged images of the isolated flagella we
438 observed the presence of *Tc*BDF3 and acetylated α tubulin in these resistant structures
439 (Figure 5A, green and red arrows heads), which further corroborated the results obtained by
440 TEM. These results suggest that *Tc*BDF3 localization correlates to acetylated α tubulin,
441 although the opposite is not necessarily true. In trypomastigotes (T), *Tc*BDF3 was present
442 only in the flagellum, as it was previously determined using intact parasites, where it co-
443 localized partially with acetylated α tubulin (Figure 5A). Localization of *Tc*BDF3 and PAR2
444 was compared in detail to determine if *Tc*BDF3 was present in the paraflagellar rod. The
445 paraflagellar rod is present from the point where the flagellum exits the flagellar pocket and
446 runs alongside the axoneme right to the distal tip. We observed that in the flagellum of
447 epimastigotes and trypomastigotes the two proteins did not co-localize but they seemed to
448 run side by side, supporting the hypothesis that *Tc*BDF3 is present in the flagellar axoneme of
449 *T. cruzi* but not in the paraflagellar rod (Figure 5B). The presence of *Tc*BDF3 but not of PAR2
450 in the flagellar pocket region is clearly observed in the enlarged images of the isolated flagella
451 (Figure 5B, green and red arrow heads).

452 Next, western blot assays with anti-*Tc*BDF3 and anti-acetylated α tubulin were performed
453 using protein extracts enriched in cytoskeletal and flagellar proteins (Figure 6A). Three
454 enriched fractions which corresponded to soluble proteins (Sn1), soluble cytoskeletal and

EC Accepts published online ahead of print

455 flagellar proteins (Sn2) and insoluble cytoskeletal and flagellar proteins (P) were obtained by
456 differential extraction with detergent as described by Schneider and co-workers (11). *Tc*BDF3
457 and acetylated α tubulin seemed to be fractionated together from soluble protein pools and
458 from insoluble flagellar and cytoskeletal protein complexes. These results suggested that the
459 interaction between these proteins is restricted to some specific cellular compartments.
460 Immuno-precipitation assays were performed to study the interaction of *Tc*BDF3 with
461 acetylated α tubulin (Figure 6B). We used anti-*Tc*BDF3 antibodies coupled to magnetic
462 beads. Both *Tc*BDF3 and acetylated α tubulin were detected by western blot analysis in the
463 immunoprecipitated complexes. These results demonstrated that these two proteins interact
464 *in vivo*. We did not detect any immunoreactive band using magnetic beads coupled to purified
465 IgG (negative control).
466 To test *Tc*BDF3 binding specificity for acetylated α tubulin, we blotted acetylated, non-
467 acetylated α tubulin (Ac α tubulin and α tubulin) and histone H4 acetylated in lysine 14
468 (H4K14Ac) peptides onto a nitrocellulose membrane. Then, the membrane was incubated
469 with recombinant *Tc*BDF3 and *Tc*BDF2 (fused to a Histidine tag) and the bound proteins were
470 visualized by western blot analysis with anti-Histidine antibodies (Figure 6C). There was no
471 cross reactivity between bromodomain factors, recombinant *Tc*BDF2 only recognized the
472 H4K14Ac peptide (25) and *Tc*BDF3 only the acetylated α tubulin peptide. This suggests that
473 each BDF can recognize and bind to one (or a limited number of) specific acetylated lysine
474 residues.
475 Although tubulin acetylation is a widespread modification present in all eukaryotic cells, its
476 precise function on cytoskeleton dynamics has not been completely elucidated yet. Recent
477 reports suggested a function for this PTM in axonemal-related cell structures. The acetylation
478 of α tubulin at K40 by the specific enzyme MEC-17 was associated to ciliogenesis and

EC Accepts published online ahead of print

479 efficient mechanosensation in *Caenorhabditis elegans* (17, 53). Trypanosomes are
480 evolutionary early-branched species that have some unique characteristics. The participation
481 of a bromodomain-containing protein complex during metacyclogenesis could also be a
482 unique feature of these particular eukaryotic cells. It has been proposed that cilia and flagella
483 emerged early in eukaryotic evolution, and that in primitive eukaryotes microtubule PTMs
484 existed as a cilia and flagella specific phenomenon, which was later adapted to other
485 microtubule structures (6).

486 The results presented herein show that *Tc*BDB3 binds to acetylated α tubulin both *ex vivo* and
487 *in vivo*. This interaction seems to be associated with changes in the amount of *Tc*BDF3 in the
488 flagellum during metacyclogenesis. Although the exact meaning of this observation cannot be
489 understood yet, it is important to mention that *Tc*BDF3 is the first described bromodomain-
490 containing protein that recognizes a modification in tubulin and, hence, the first candidate to
491 be able to read a tubulin PTM. At least two basic models can be proposed for its mode of
492 action. In analogy to those already proposed for histone-binding bromodomains, a *Tc*BDF3-
493 containg complex could be carrying an enzymatic activity to the flagellum to modify tubulin or
494 any other cytoskeletal component. Another hypothesis is that *Tc*BDF3 might carry acetylated
495 α tubulin from the cell body to the flagellum. However, we cannot rule out the possibility that
496 *Tc*BDF3 simply binds to the acetylated lysine residue to protect it from the action of modifying
497 enzymes.

498 A bromodomain-containing protein complex involved in the remodelling of the cytoskeleton in
499 *T. cruzi* may also be a new quimotherapeutic target for Chagas' disease. Recently, two
500 inhibitors that target bromodomains from the BET family have shown selective activity in a
501 squamous cell carcinoma model (54). Many other inhibitors of the bromodomain-acetyl lysine
502 interaction were developed later, putting bromodomains alongside KATs (Lysine

503 Acetyltransferases) and KDACs (Lysine Deacetylases) as interesting targets for diseases
504 caused by aberrant acetylation of lysine residues (55). The presence of an exclusively
505 cytoplasmic bromodomain, as *Tc*BDF3, could be another feature of trypanosomatids absent
506 in mammalian host cells and hence could be considered as potential targets for the
507 development of new drugs against trypanosomiasis.

508

509 **Acknowledgements**

510 This work was supported by the National Research Council (CONICET) grant PIP2010-0685
511 and the National Agency of Scientific and Technological Promotion (ANPCyT) and Glaxo
512 SmithKline joint grant PICTO2011-0046.

513 V.L Alonso, and C. Ritagliati are fellows and E.C. Serra, P. Cribb and G.V. Villanova are
514 researchers of the National Research Council (CONICET), Argentina.

515 Authors would like to thank to Dr. K. Gull for his generous gift of anti-*T. brucei* α tubulin
516 antibodies; Dr. C. Nowiki for the anti-*T. cruzi* Tyrosine Amino Transferase and anti-*T.cruzi*
517 Malate Dehydrogenase antibodies; Dr. A. Silver for the anti-PAR2 antibodies; Dr. Sergio
518 Schenkman for the anti-Histone H4 antibodies and H4K14 acetylated peptides, and Dr.
519 Lisvane Silva for helping to rise the mouse anti-*Tc*BDF3 antisera.

520
521
522
523
524
525
526
527
528

EC Accepts published online ahead of print

EC Accepts published online ahead of print

529 References

530

531 1. **Contreras VT, Araujo-Jorge TC, Bonaldo MC, Thomaz N, Barbosa HS, Meirelles Mde N,**
532 **Goldenberg S.** 1988. Biological aspects of the Dm 28c clone of Trypanosoma cruzi after
533 metacyclogenesis in chemically defined media. Mem Inst Oswaldo Cruz **83:**123-133.
534 2. **Hill KL.** 2010. Parasites in motion: flagellum-driven cell motility in African trypanosomes. Curr
535 Opin Microbiol **13:**459-465.
536 3. **Field MC, Carrington M.** 2009. The trypanosome flagellar pocket. Nat Rev Microbiol **7:**775-
537 786.
538 4. **Hammond JW, Cai D, Verhey KJ.** 2008. Tubulin modifications and their cellular functions.
539 Curr Opin Cell Biol **20:**71-76.
540 5. **Verhey KJ, Gaertig J.** 2007. The tubulin code. Cell Cycle **6:**2152-2160.
541 6. **Janke C, Bulinski JC.** 2011. Post-translational regulation of the microtubule cytoskeleton:
542 mechanisms and functions. Nat Rev Mol Cell Biol **12:**773-786.
543 7. **Cambray-Deakin MA, Burgoyne RD.** 1987. Acetylated and detyrosinated alpha-tubulins are
544 co-localized in stable microtubules in rat meningeal fibroblasts. Cell Motil Cytoskeleton **8:**284-
545 291.
546 8. **Belmadani S, Pous C, Fischmeister R, Mery PF.** 2004. Post-translational modifications of
547 tubulin and microtubule stability in adult rat ventricular myocytes and immortalized HL-1
548 cardiomyocytes. Mol Cell Biochem **258:**35-48.
549 9. **Janke C, Kneussel M.** 2010. Tubulin post-translational modifications: encoding functions on
550 the neuronal microtubule cytoskeleton. Trends Neurosci **33:**362-372.
551 10. **Souto-Padron T, Cunha e Silva NL, de Souza W.** 1993. Acetylated alpha-tubulin in
552 Trypanosoma cruzi: immunocytochemical localization. Mem Inst Oswaldo Cruz **88:**517-528.
553 11. **Schneider A, Sherwin T, Sasse R, Russell DG, Gull K, Seebeck T.** 1987. Subpellicular and
554 flagellar microtubules of Trypanosoma brucei brucei contain the same alpha-tubulin isoforms. J
555 Cell Biol **104:**431-438.

EC Accepts published online ahead of print

556 12. **Alonso VL, Serra EC.** 2012. Lysine acetylation: elucidating the components of an emerging
557 global signaling pathway in trypanosomes. J Biomed Biotechnol **2012:**452934.
558 13. **Hubbert C, Guardiola A, Shao R, Kawaguchi Y, Ito A, Nixon A, Yoshida M, Wang XF, Yao**
559 **TP.** 2002. HDAC6 is a microtubule-associated deacetylase. Nature **417:**455-458.
560 14. **North BJ, Marshall BL, Borra MT, Denu JM, Verdin E.** 2003. The human Sir2 ortholog,
561 SIRT2, is an NAD+-dependent tubulin deacetylase. Mol Cell **11:**437-444.
562 15. **Tavares J, Ouaissi A, Santarem N, Sereno D, Vergnes B, Sampaio P, Cordeiro-da-Silva**
563 **A.** 2008. The Leishmania infantum cytosolic SIR2-related protein 1 (LiSIR2RP1) is an NAD+ -
564 dependent deacetylase and ADP-ribosyltransferase. Biochem J **415:**377-386.
565 16. **Creppe C, Malinouskaya L, Volvert ML, Gillard M, Close P, Malaise O, Laguesse S,**
566 **Cornez I, Rahmouni S, Ormenese S, Belachew S, Malgrange B, Chapelle JP, Siebenlist**
567 **U, Moonen G, Chariot A, Nguyen L.** 2009. Elongator controls the migration and differentiation
568 of cortical neurons through acetylation of alpha-tubulin. Cell **136:**551-564.
569 17. **Shida T, Cueva JG, Xu Z, Goodman MB, Nachury MV.** 2010. The major {alpha}-tubulin K40
570 acetyltransferase {alpha}TAT1 promotes rapid ciliogenesis and efficient mechanosensation.
571 Proc Natl Acad Sci U S A.
572 18. **Alsford S, Horn D.** 2011. Elongator protein 3b negatively regulates ribosomal DNA
573 transcription in african trypanosomes. Mol Cell Biol **31:**1822-1832.
574 19. **Zeng L, Zhou MM.** 2002. Bromodomain: an acetyl-lysine binding domain. FEBS Lett **513:**124-
575 128.
576 20. **Yang XJ.** 2004. Lysine acetylation and the bromodomain: a new partnership for signaling.
577 Bioessays **26:**1076-1087.
578 21. **Crowley T, Brunori M, Rhee K, Wang X, Wolgemuth DJ.** 2004. Change in nuclear-
579 cytoplasmic localization of a double-bromodomain protein during proliferation and
580 differentiation of mouse spinal cord and dorsal root ganglia. Brain Res Dev Brain Res **149:**93-
581 101.

EC Accepts published online ahead of print

582 22. **Crowley TE, Kaine EM, Yoshida M, Nandi A, Wolgemuth DJ.** 2002. Reproductive cycle
583 regulation of nuclear import, euchromatic localization, and association with components of Pol
584 II mediator of a mammalian double-bromodomain protein. Mol Endocrinol **16:**1727-1737.
585 23. **Trousdale RK, Wolgemuth DJ.** 2004. Bromodomain containing 2 (Brd2) is expressed in
586 distinct patterns during ovarian folliculogenesis independent of FSH or GDF9 action. Mol
587 Reprod Dev **68:**261-268.
588 24. **Ivens AC, Peacock CS, Worthey EA, Murphy L, Aggarwal G, Berriman M, Sisk E,
589 Rajandream MA, Adlem E, Aert R, Anupama A, Apostolou Z, Attipoe P, Bason N, Bauser
590 C, Beck A, Beverley SM, Bianchettin G, Borzym K, Bothe G, Bruschi CV, Collins M,
591 Cadag E, Ciarloni L, Clayton C, Coulson RM, Cronin A, Cruz AK, Davies RM, De
592 Gaudenzi J, Dobson DE, Duesterhoeft A, Fazelina G, Fosker N, Frasch AC, Fraser A,
593 Fuchs M, Gabel C, Goble A, Goffeau A, Harris D, Hertz-Fowler C, Hilbert H, Horn D,
594 Huang Y, Klages S, Knights A, Kube M, Larke N, Litvin L, Lord A, Louie T, Marra M,
595 Masuy D, Matthews K, Michaeli S, Mottram JC, Muller-Auer S, Munden H, Nelson S,
596 Norbertczak H, Oliver K, O'Neil S, Pentony M, Pohl TM, Price C, Purnelle B, Quail MA,
597 Rabbinowitsch E, Reinhardt R, Rieger M, Rinta J, Robben J, Robertson L, Ruiz JC,
598 Rutter S, Saunders D, Schafer M, Schein J, Schwartz DC, Seeger K, Seyler A, Sharp S,
599 Shin H, Sivam D, Squares R, Squares S, Tosato V, Vogt C, Volckaert G, Wambutt R,
600 Warren T, Wedler H, Woodward J, Zhou S, Zimmermann W, Smith DF, Blackwell JM,
601 Stuart KD, Barrell B, Myler PJ.** 2005. The genome of the kinetoplastid parasite, Leishmania
602 major. Science **309:**436-442.
603 25. **Villanova GV, Nardelli SC, Cribb P, Magdaleno A, Silber AM, Motta MC, Schenkman S,
604 Serra E.** 2009. Trypanosoma cruzi bromodomain factor 2 (BDF2) binds to acetylated histones
605 and is accumulated after UV irradiation. Int J Parasitol **39:**665-673.

EC Accepts published online ahead of print

606 26. **Camargo ME, Segura EL, Kagan IG, Souza JM, Carvalheiro Jda R, Yanovsky JF,**
607 **Guimaraes MC.** 1986. Three years of collaboration on the standardization of Chagas' disease
608 serodiagnosis in the Americas: an appraisal. Bull Pan Am Health Organ **20:**233-244.
609 27. **Tonelli RR, Silber AM, Almeida-de-Faria M, Hirata IY, Colli W, Alves MJ.** 2004. L-proline is
610 essential for the intracellular differentiation of Trypanosoma cruzi. Cell Microbiol **6:**733-741.
611 28. **Yoshida N, Mortara RA, Araguth MF, Gonzalez JC, Russo M.** 1989. Metacyclic neutralizing
612 effect of monoclonal antibody 10D8 directed to the 35- and 50-kilodalton surface
613 glycoconjugates of Trypanosoma cruzi. Infect Immun **57:**1663-1667.
614 29. **Batista M, Marchini FK, Celedon PA, Fragoso SP, Probst CM, Preti H, Ozaki LS, Buck**
615 **GA, Goldenberg S, Krieger MA.** 2010. A high-throughput cloning system for reverse genetics
616 in Trypanosoma cruzi. BMC Microbiol **10:**259.
617 30. **Cribb P, Perozzi M, Villanova GV, Trochine A, Serra E.** 2011. Characterization of TcHMGB,
618 a high mobility group B family member protein from Trypanosoma cruzi. Int J Parasitol
619 **41:**1149-1156.
620 31. **da Cunha JP, Nakayasu ES, de Almeida IC, Schenkman S.** 2006. Post-translational
621 modifications of Trypanosoma cruzi histone H4. Mol Biochem Parasitol **150:**268-277.
622 32. **Rasband WS.** 1997-2011. ImageJ software. *In* U. S. National Institutes of Health B, Maryland,
623 USA (ed.), http://imagej.nih.gov/ij/.
624 33. **Sasse R, Gull K.** 1988. Tubulin post-translational modifications and the construction of
625 microtubular organelles in Trypanosoma brucei. J Cell Sci **90 (Pt 4):**577-589.
626 34. **Kelley LA, Sternberg MJ.** 2009. Protein structure prediction on the Web: a case study using
627 the Phyre server. Nat Protoc **4:**363-371.
628 35. **Zhang X, Shen Y, Ding G, Tian Y, Liu Z, Li B, Wang Y, Jiang C.** 2013. TFPP: an SVM-
629 based tool for recognizing flagellar proteins in Trypanosoma brucei. PLoS One **8:**e54032.

EC Accepts published online ahead of print

630 36. **Broadhead R, Dawe HR, Farr H, Griffiths S, Hart SR, Portman N, Shaw MK, Ginger ML,**
631 **Gaskell SJ, McKean PG, Gull K.** 2006. Flagellar motility is required for the viability of the
632 bloodstream trypanosome. Nature **440:**224-227.
633 37. **Hart SR, Lau KW, Hao Z, Broadhead R, Portman N, Huhmer A, Gull K, McKean PG,**
634 **Hubbard SJ, Gaskell SJ.** 2009. Analysis of the trypanosome flagellar proteome using a
635 combined electron transfer/collisionally activated dissociation strategy. J Am Soc Mass
636 Spectrom **20:**167-175.
637 38. **Oberholzer M, Langousis G, Nguyen HT, Saada EA, Shimogawa MM, Jonsson ZO,**
638 **Nguyen SM, Wohlschlegel JA, Hill KL.** 2011. Independent analysis of the flagellum surface
639 and matrix proteomes provides insight into flagellum signaling in mammalian-infectious
640 Trypanosoma brucei. Mol Cell Proteomics **10:**M111 010538.
641 39. **Nowicki C, Montemartini M, Duschak V, Santome JA, Cazzulo JJ.** 1992. Presence and
642 subcellular localization of tyrosine aminotransferase and p-hydroxyphenyllactate
643 dehydrogenase in epimastigotes of Trypanosoma cruzi. FEMS Microbiol Lett **71:**119-124.
644 40. **Marciano D, Maugeri DA, Cazzulo JJ, Nowicki C.** 2009. Functional characterization of stage-
645 specific aminotransferases from trypanosomatids. Mol Biochem Parasitol **166:**172-182.
646 41. **Marciano D, Llorente C, Maugeri DA, de la Fuente C, Opperdoes F, Cazzulo JJ, Nowicki**
647 **C.** 2008. Biochemical characterization of stage-specific isoforms of aspartate
648 aminotransferases from Trypanosoma cruzi and Trypanosoma brucei. Mol Biochem Parasitol
649 **161:**12-20.
650 42. **Choudhary C, Kumar C, Gnad F, Nielsen ML, Rehman M, Walther TC, Olsen JV, Mann M.**
651 2009. Lysine acetylation targets protein complexes and co-regulates major cellular functions.
652 Science **325:**834-840.
653 43. **Kim SC, Sprung R, Chen Y, Xu Y, Ball H, Pei J, Cheng T, Kho Y, Xiao H, Xiao L, Grishin**
654 **NV, White M, Yang XJ, Zhao Y.** 2006. Substrate and functional diversity of lysine acetylation
655 revealed by a proteomics survey. Mol Cell **23:**607-618.

EC Accepts published online ahead of print

656 44. **Yu BJ, Kim JA, Moon JH, Ryu SE, Pan JG.** 2008. The diversity of lysine-acetylated proteins
657 in Escherichia coli. J Microbiol Biotechnol **18:**1529-1536.
658 45. **Zhao S, Xu W, Jiang W, Yu W, Lin Y, Zhang T, Yao J, Zhou L, Zeng Y, Li H, Li Y, Shi J, An**
659 **W, Hancock SM, He F, Qin L, Chin J, Yang P, Chen X, Lei Q, Xiong Y, Guan KL.** 2010.
660 Regulation of cellular metabolism by protein lysine acetylation. Science **327:**1000-1004.
661 46. **Kouzarides T.** 2000. Acetylation: a regulatory modification to rival phosphorylation? EMBO J
662 **19:**1176-1179.
663 47. **Polevoda B, Sherman F.** 2002. The diversity of acetylated proteins. Genome Biol
664 **3:**reviews0006.
665 48. **Norvell A, McMahon SB.** 2010. Cell biology. Rise of the rival. Science **327:**964-965.
666 49. **Close P, Creppe C, Gillard M, Ladang A, Chapelle JP, Nguyen L, Chariot A.** 2010. The
667 emerging role of lysine acetylation of non-nuclear proteins. Cell Mol Life Sci **67:**1255-1264.
668 50. **Kim GW, Yang XJ.** 2010. Comprehensive lysine acetylomes emerging from bacteria to
669 humans. Trends Biochem Sci **36:**211-220.
670 51. **Ferreira LR, Dossin Fde M, Ramos TC, Freymuller E, Schenkman S.** 2008. Active
671 transcription and ultrastructural changes during Trypanosoma cruzi metacyclogenesis. An
672 Acad Bras Cienc **80:**157-166.
673 52. **Kohl L, Gull K.** 1998. Molecular architecture of the trypanosome cytoskeleton. Mol Biochem
674 Parasitol **93:**1-9.
675 53. **Akella JS, Wloga D, Kim J, Starostina NG, Lyons-Abbott S, Morrissette NS, Dougan ST,**
676 **Kipreos ET, Gaertig J.** 2010. MEC-17 is an alpha-tubulin acetyltransferase. Nature **467:**218-
677 222.
678 54. **Filippakopoulos P, Qi J, Picaud S, Shen Y, Smith WB, Fedorov O, Morse EM, Keates T,**
679 **Hickman TT, Felletar I, Philpott M, Munro S, McKeown MR, Wang Y, Christie AL, West N,**
680 **Cameron MJ, Schwartz B, Heightman TD, La Thangue N, French CA, Wiest O, Kung AL,**

EC Accepts published online ahead of print

681 **Knapp S, Bradner JE.** 2010. Selective inhibition of BET bromodomains. Nature **468:**1067-
682 1073.
683 55. **Muller S, Filippakopoulos P, Knapp S.** 2011. Bromodomains as therapeutic targets. Expert
684 Rev Mol Med **13:**e29.
685

686 **Figure 1: *Tc*BDF3 is a cytoplasmatic bromodomain-containing protein in
687 epimastigotes.** (A) Nuclear (N) and Non-nuclear (NN) protein extracts (30 μg per well) were
688 subjected to western blot analysis using rabbit anti-*Tc*BDF3 antibodies, anti-Tyrosine
689 aminotransferase (*Tc*TAT) (cytosolic), anti-*T.cruzi* High Mobility Group B (*Tc*HMGB) (nuclear),
690 anti-*T.cruzi* Bromodomain Factor 2 (*Tc*BDF2) (nuclear) and anti-*T.cruzi* H4 histone (*Tc*H4)
691 (nuclear). The first panel shows the Coomassie-stained gel. (B) Enzymatic activity of Alpha
692 Hydroxyacid Dehydrogenase (aHAdH) and Malate Dehydrogenase (MdH) in epimastigotes
693 treated with increasing concentrations of digitonin. Activities were measured and normalized
694 to the protein concentration in the extracts. The arrows below the graph indicate the digitonin
695 concentration at which cytosolic (C) glycosomal (G) and mitochondrial (M) proteins are
696 released. (C) Equal volumes of selected soluble (S) and insoluble (P) fractions obtained at
697 different digitonin amounts (0-0.7 mg) were subjected to western blot analysis using anti-
698 *Tc*BDF3 antibodies (*Tc*BDF3) and known markers for different organelles. The antibodies
699 used were: anti-*T. cruzi* Tyrosine Amino Transferase (*Tc*TAT) (cytosolic), anti-*T. cruzi*
700 glycosomal Malate Dehydrogenase (*Tc*MdHglyc) (glycosomal), anti-*T. cruzi* mitochondrial
701 Malate Dehidrogenase (*Tc*MdHmit) (mitochondrial), anti-*T. cruzi* paraflagellar rod 2 protein
702 (*Tc*PAR2) (flagellar) and anti-α tubulin (α tubulin) (cytoskeletal). TL, total lisate.
703

EC Accepts published online ahead of print

704 **Figure 2: *Tc*BDF3 is localized at the cytoplasm, the flagellum and the flagellar pocket of**
705 **epimastigotes.** (A-E) Immunoelectron microscopy of *Tc*BDF3 in *T. cruzi* epimastigotes using
706 purified rabbit anti-*Tc*BDF3 antibodies. The nucleus (N), kinetoplast (K), flagellar pocket (FP)
707 and flagellum (F) are indicated. Gold particles are indicated with black and white arrows.
708 White arrows indicate flagellar labelling. (D) Enlarged image of the marked area in (C). (F)
709 Enlarged image of the marked area in (E). Bar = 1 μm.
710
711 **Figure 3: *Tc*BDF3 is expressed throughout the *T. cruzi* life cycle *in vitro*.** (A) Western
712 blot analysis using purified rabbit anti-*Tc*BDF3 antibodies (*a*-*Tc*BDF3) and mouse anti-α
713 tubulin (*a*-α tubulin) as a loading control. A, amastigotes total protein extracts; E,
714 epimastigotes total protein extracts; T, trypomastigotes total protein extracts (30 μg per well).
715 (B) Immuno-fluorescence assay using purified anti-*Tc*BDF3 and parasites at different stages
716 of the *T. cruzi* life cycle. A, free amastigote; Ac, amastigotes inside a Vero cell; E,
717 epimastigote; T, trypomastigote from infected Vero cells; Tm, metacyclic trypomastigote
718 obtained *in vitro*. Anti-rabbit IgG conjugated to Fluorescein was used as secondary antibody.
719 Nucleus and kinetoplast were labelled with DAPI. Bars = 2 μm.
720
721 **Figure 4: *Tc*BDF3 changes its location during *in vitro* metacyclogenesis.**
722 Immunofluorescence assays using purified rabbit anti-*Tc*BDF3 (*a*-*Tc*BDF3) and mouse
723 monoclonal anti-acetylated α tubulin (*a*-AcTub) antibodies in intermediate stages 1a, 1b and
724 1c as defiened by (51). On the right side a schematic diagram of the position of the flagellum
725 (F), nucleus (N) and kinetoplast (K) in the three selected intermediate differentiation stages is
726 shown. Anti-rabbit IgG conjugated to Fluorescein (green) and anti-mouse IgG conjugated to

727 Rodhamine (red) were used as secondary antibodies. Nucleus and kinetoplast were labelled
728 with DAPI (blue).
729
730 **Figure 5: *Tc*BDF3 is detected in the cytoskeleton and flagellum of epimastigotes and**
731 **only in the flagellum of metacyclic trypomastigotes.** Immunofluorescence assays using
732 purified rabbit anti-*Tc*BDF3 (*a*-*Tc*BDF3), mouse monoclonal anti-acetylated α tubulin (*a*-
733 AcTub) (A) and mouse anti-PAR2 (*a*-PFR) (B) antibodies on isolated cytoskeletons and
734 flagella of epimastigotes and metacyclic trypomastigotes. Anti-rabbit IgG conjugated to
735 Fluorescein (green) and anti-mouse IgG conjugated to Rodhamine (red) were used as
736 secondary antibodies. Panels on the right of A and B show enlarged images of the detergent
737 resistant structures that correspond to MTs attached to basal bodies and forming the flagellar
738 pocket. Green arrow heads show *Tc*BDF3 localization and red arrow heads show acetylated
739 α tubulin (A) and PAR2 (B) localization in these structures.
740
741 **Figure 6: *Tc*BDF3 interacts with acetylated α tubulin.** (A) Coomassie stained SDS-PAGE
742 and western blot analysis of epimastigotes protein extracts enriched in cytoskeletal and
743 flagellar proteins. Sn1, soluble protein extracts; Sn2, soluble cytoskeletal and flagellar protein
744 extracts; P, insoluble cytoskeletal and flagellar protein extracts (50 μg per well). Rabbit anti-
745 *Tc*BDF3 antibodies (*a*-*Tc*BDF3) and mouse anti-acetylated α tubulin antibodies (*a*-AcTub)
746 were used. (B) Co-immunoprecipitation assay using purified anti-*Tc*BDF3 antibodies
747 covalently coupled to magnetic beads (*Tc*BDF3 beads). Magnetic beads coupled to IgGs
748 (purified from antisera of non-immunized rabbits) were used as a negative control (Control
749 beads). Left panel shows a silver stained SDS-PAGE of total cytoskeletal extracts and the
750 elutions obtained after the immunoprecipitation experiment. Right panel shows a western blot

EC Accepts published online ahead of print

751 analysis of the eluted proteins after coimmunoprecipitation using purified rabbit anti-*Tc*BDF3
752 antibodies (*a*-*Tc*BDF3) and mouse monoclonal anti-acetylated α tubulin antibodies (*a*-AcTub).
753 (C) Slot far western blot assay. Acetylated tubulin (TubK40Ac), non-acetylated tubulin (Tub)
754 or acetylated histone H4 (H4K14Ac) peptides were blotted onto a nitrocellulose membrane
755 and incubated with His-tagged recombinant *Tc*BDF3 (BDF3-His) or *Tc*BDF2 (BDF2-His).
756 Bound recombinant proteins were detected with anti-Histidine antibodies (*a*-His). Signals
757 were quantified by densitometry and normalized using the interaction with acetylated α tubulin
758 peptide as a reference (assigned the arbitrary value of 1). Error bars indicate means ± S.D.
759 from results of three independent experiments.
760

761

EC Accepts published online ahead of print

EC Accepts published online ahead of print

A

MW N NN N NN N NN N NN N NN N NN

116
66.2
45
35
25
18.4

*Tc*BDF3 *Tc*TAT *Tc*HMGB *Tc*BDF2 *Tc*H4

B

Enzymatic activity (%)

100
80
60
40
20
0

0.0 0.1 0.2 0.3 0.4 0.5 0.6 0.7 0.8 0.9 1.0

Digitonin (mg)

aHAdH
MdH

C
G
M

C

Selected Fractions

0 0.04 0.12 0.20 0.28 0.40 0.54 0.7 TL

0 0.04 0.12 0.20 0.28 0.40 0.54 0.7 TL Digotonin (mg)

*Tc*TAT S P

*Tc*MdHglyc S P

*Tc*MdHmit S P

S P *Tc*BDF3

S P α tubulin

S P *Tc*PAR2

EC Accepts published online ahead of print

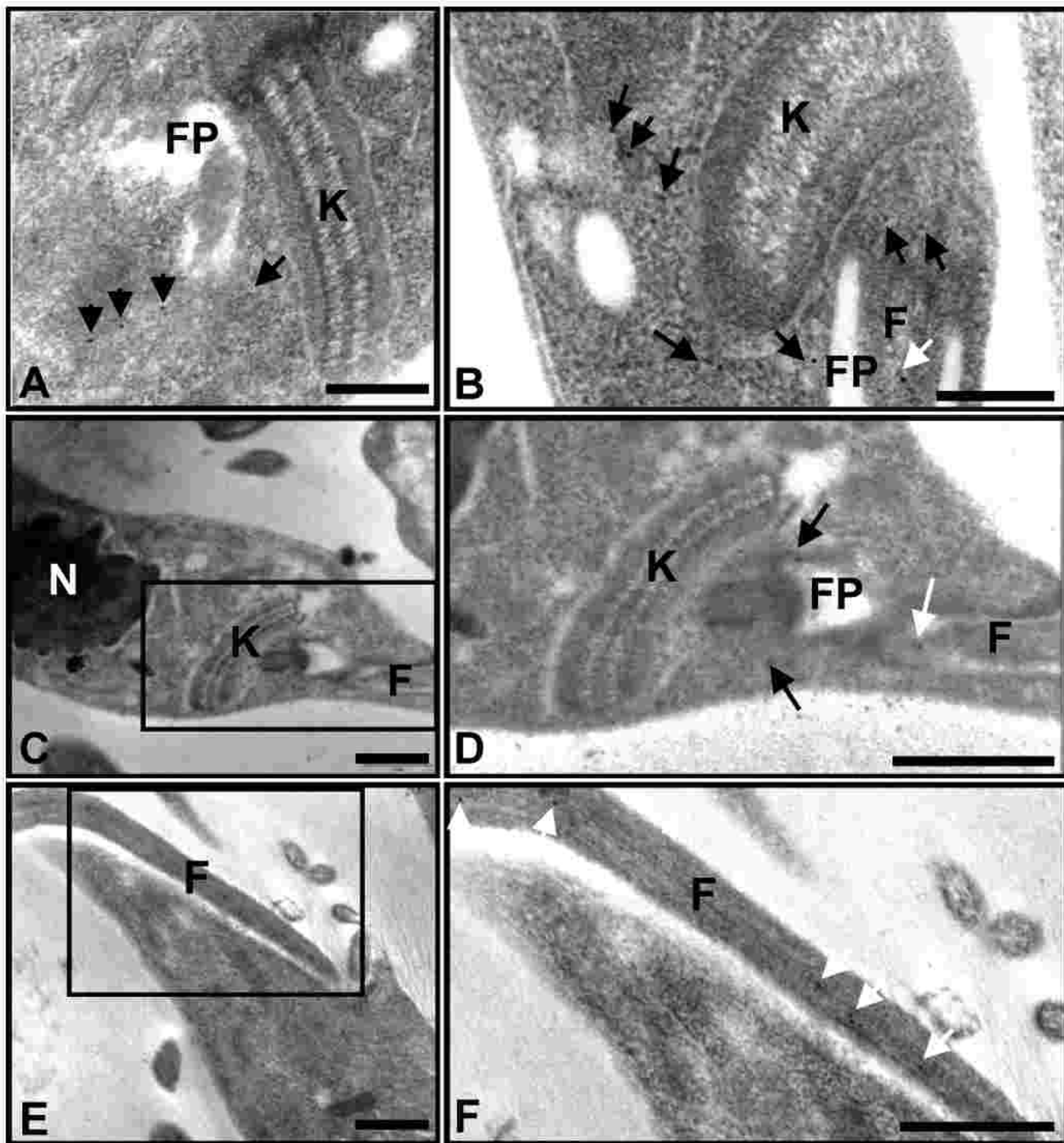

EC Accepts published online ahead of print

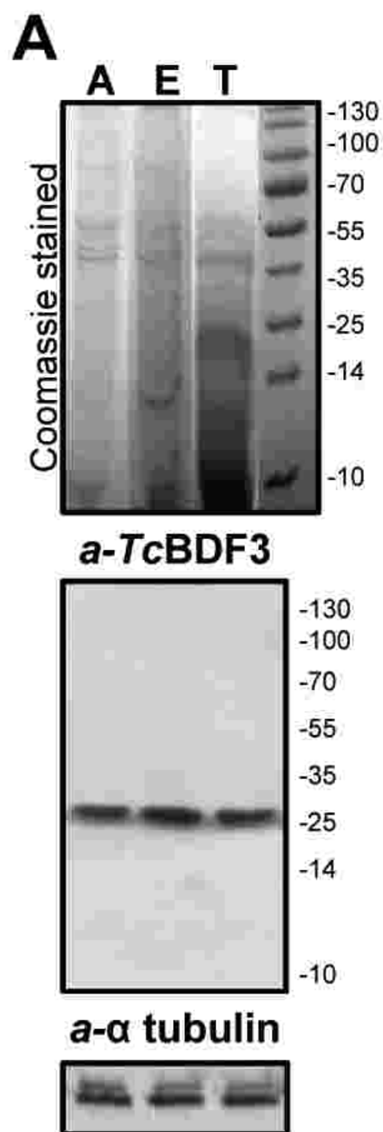

EC Accepts published online ahead of print

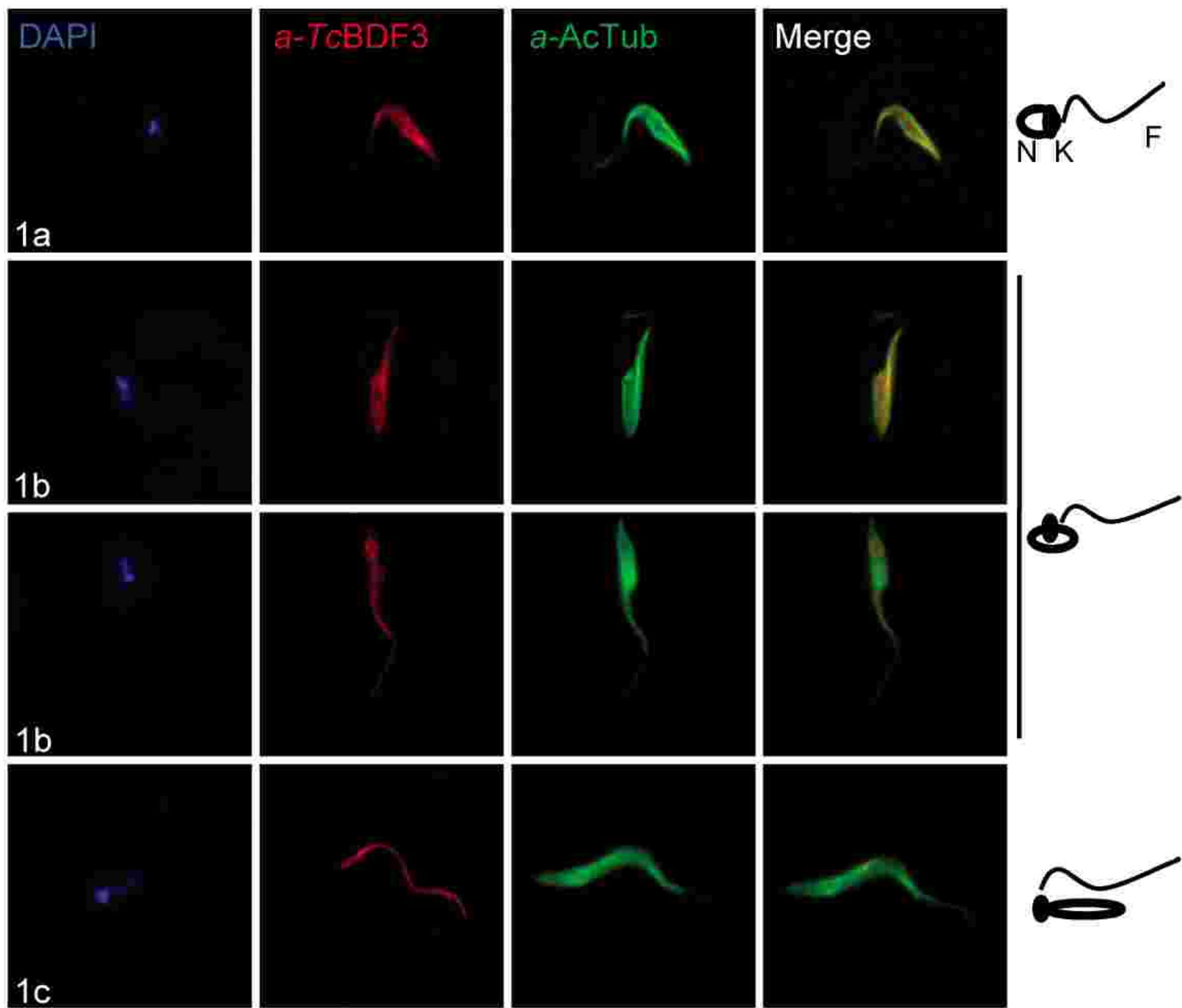

EC Accepts published online ahead of print

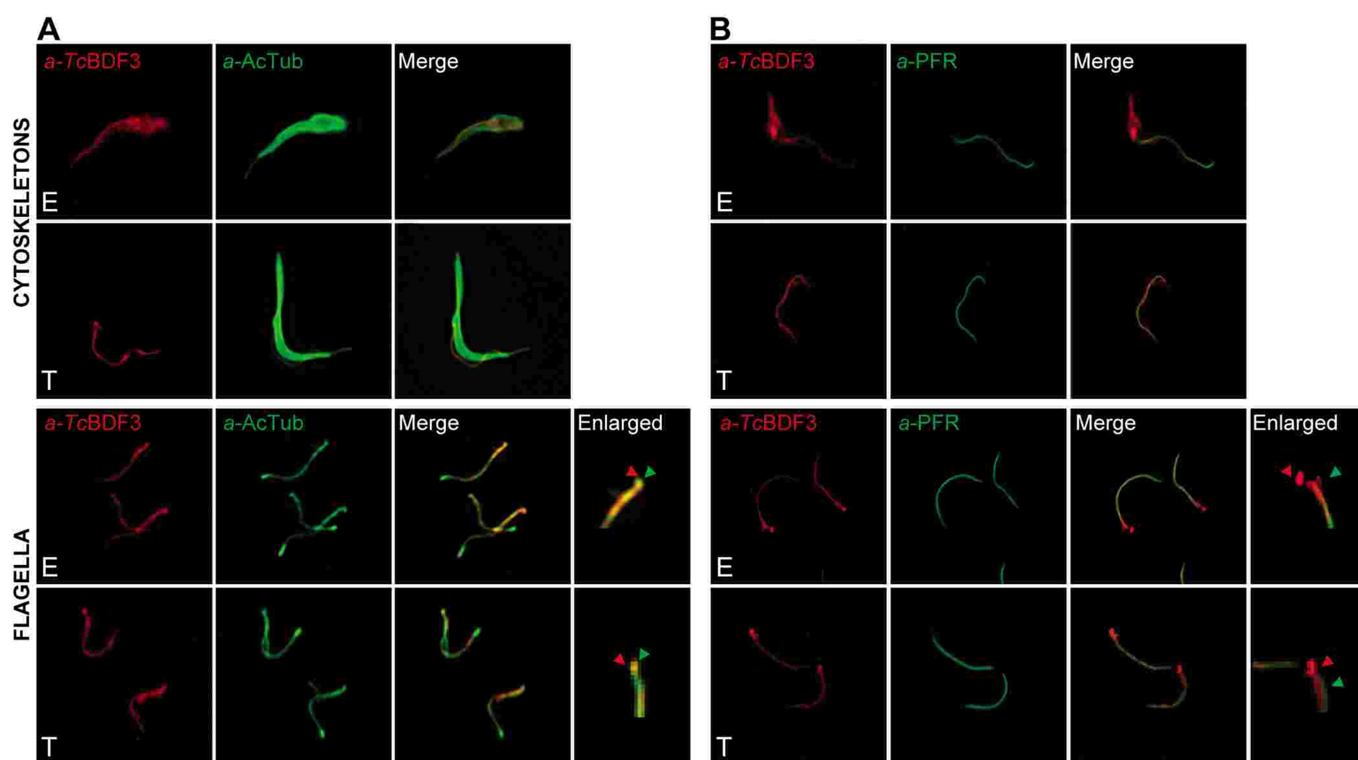

EC Accepts published online ahead of print